AIP Journal of Applied Physics

Iterative approaches describing atomic diffusion in finite single- and two-phase systems

C. R. Houska and J. Unnam

Citation: Journal of Applied Physics **47**, 4325 (1976); doi: 10.1063/1.322434
View online: http://dx.doi.org/10.1063/1.322434
View Table of Contents: http://scitation.aip.org/content/aip/journal/jap/47/10?ver=pdfcov
Published by the AIP Publishing

Iterative approaches describing atomic diffusion in finite single- and two-phase systems

C. R. Houska and J. Unnam

Department of Materials Engineering, Virginia Polytechnic Institute and State University, Blacksburg Virginia 24061

(Received 22 March 1976)

Iterative solutions are given for planar one-dimensional atomic diffusion in finite single- and two-phase systems. They are usable for any continuous variation of the interdiffusion coefficient $D(C)$ within each phase, and need not be fitted to special functions such as a power series or an exponential function. Modified integral functions similar to one first proposed by Boltzmann are used along with a conservation criterion to locate the interface position ξ. Computer time for the iterative solutions is about two to three magnitudes shorter than finite-difference (F-D) calculations because of the rapid convergence of the integral equations. The accuracy of these approximate forms is considered. Excellent agreement was obtained between F-D calculations and the iterative approach for semi-infinite single-phase systems. Good agreement is also found for two-phase systems; however, the accuracy varies with the solubility gap size $C_{\beta a} - C_{a\beta}$. The best results are obtained for gaps larger than 0.7 which includes most eutectic systems. Calculations of composition profiles which are based upon the maximum solid solubilities for the Cu-Ag system are within 1% of the F-D calculations.

PACS numbers: 66.30.Fq, 68.50.+j, 64.80.Cz

I. INTRODUCTION

It has been reported that for those cases where atomic species are being transferred across phase boundaries, the interfacial compositions at the boundaries could not be exactly the equilibrium values given by the constitutional diagram.[1] The actual values may vary continuously during the course of diffusion. For many systems the equilibrium concentrations are closely approached in a time period which is small relative to the over-all experimental time, and under such conditions the transformation is treated as diffusion controlled. We will treat approximate solutions giving the concentration profile for finite and semifinite two-phase diffusion-controlled systems. For these cases, the surface composition will vary with time during a later stage of the diffusion treatment. A planar iterative solution describing the finite case is given in which the interdiffusion coefficient $D(C)$ is allowed to vary separately for each phase without necessarily assuming special forms.

Thus far, no closed-form solutions are available for the case of variable $D(C)$ in which one or two of the phases is finite. In this case, a planar interface may reverse its direction after first moving into the substrate. Or, it may move toward the free surface without reversal depending upon the interface flux balance. This was demonstrated with finite-difference calculations under a large range of conditions[2] using constant diffusion coefficients for each phase. A similar reversal was demonstrated using closed-form solutions and constant diffusion coefficients.[3,4] The authors have also employed finite-difference calculations to determine the interface position and composition profiles for each phase. However, excessive computer time is required to obtain accurate solutions without spurious oscillations if one phase is finite and the other infinite in thickness. Hours of computer time are required with an IBM 370 system for only a partial mapping of the composition profiles. Consequently, we initiated a search for accurate approximations requiring computer times less than a minute, thereby enabling one to make use of a time-sharing operation. This would enable diffusion coefficients to be obtained quickly with the aid of a graphics computer terminal such as the Tektronix 4010. One simply adjusts the diffusion coefficients to fit the experimental composition profiles. Experimental results obtained by this method are given in the following paper, while the iterative diffusion equations are introduced here.

II. SINGLE-PHASE SOLUTIONS

Exact solutions of the diffusion equation can be obtained for a variety of initial and boundary conditions provided the diffusion coefficient is constant. Solutions are presented in textbooks by Crank[5] and Jost,[6] and analogous treatments are to be found in works on heat conduction such as Carslaw and Jaeger.[7] A one-dimensional solution of Fick's second law was described by Boltzmann,[8,9] which gives the concentration distribution for any continuous variation of the diffusion coefficient. This requires the diffusion geometry to be planar and the system to be doubly infinite in size. The final result is obtained by integrating Fick's second law as an ordinary differential equation after applying the Boltzmann transformation. And the resultant integral equation is solved by successive numerical integrations on a digital computer. It will be demonstrated that this solution can be successfully extended to a finite plating with a time-varying surface concentration. The Boltzmann solution represents a very general form which gives the concentration profile at any given instant of time. This equation is basic to subsequent developments and is not well known.

The nonlinear one-dimensional form for Fick's second law is given by

$$\frac{\partial C}{\partial t} = \frac{\partial}{\partial y}\left(D(C)\,\frac{\partial C}{\partial y}\right), \tag{1}$$

where the concentration is both a function of y (the distance from the Matano interface) and time t. $D(C)$ is

the variable interdiffusion coefficient. For this case, it is assumed that the system is doubly infinite. Therefore, the Boltzmann transformation may be applied to Eq. (1)

$$\nu = y/2t^{1/2} \tag{2}$$

giving the ordinary differential equation

$$-2\nu \frac{dC}{d\nu} = \frac{d}{d\nu}\left(D(C)\frac{dC}{d\nu}\right). \tag{3}$$

The boundary conditions are for $t > 0$,

$C = 1$ for $\nu \to -\infty$,

$C = 0$ for $\nu \to +\infty$,

and for $t = 0$,

$C = 1$ for $y < 0$,

$C = 0$ for $y > 0$.

By integrating Eq. (3) twice, one obtains

$$C(\nu) = 1 - \left[\int_{-\infty}^{\nu} \frac{1}{D(C)} \exp\left(-\int_{-\infty}^{\nu'} \frac{2\nu''}{D(C)}\, d\nu''\right) d\nu'\right] \times \left[\int_{-\infty}^{\infty} \frac{1}{D(C)} \exp\left(-\int_{-\infty}^{\nu'} \frac{2\nu''}{D(C)}\, d\nu''\right) d\nu'\right]^{-1}. \tag{4}$$

If $D(C)$ is constant and equal to $\langle D\rangle$, Eq. (4) goes to the well-known error function

$$C(\nu) = \tfrac{1}{2}[1 - \mathrm{erf}(\nu/\langle D\rangle^{1/2})]. \tag{5}$$

In order to find solutions to Eq. (4), it is necessary to use an iterative approach. One begins this procedure knowing $D(C)$ from experiment and by assuming a first approximation to $C(\nu)$. A first approximation to the composition profile is given by Eq. (5) where $\langle D\rangle$ is the average diffusion coefficient. The calculation of $C(\nu)$ from Eq. (4) has been programmed for an IBM 370 computer. Values of $z = \nu/\langle D\rangle^{1/2}$ ranging from -3.5 to $+3.5$ were chosen in steps of 0.1. Since $\mathrm{erf}(\pm 3.5)$ is unity to within four decimal places, this is a practical representation of the range $-\infty$ to $+\infty$. The iteration is carried out as follows:

(1) Determine C from a corresponding set of ν (or y) values using Eq. (5).

(2) With known $D(C)$, evaluate an improved set of $C(\nu)$ values using Eq. (4).

(3) Using these improved $C(\nu)$, redetermine $D(\nu)$ and recalculate C from Eq. (4).

(4) Continue the iteration until two successive approximations are within the desired accuracy.

Four or five iterations are usually sufficient to obtain a high degree of accuracy. This approach has been used in studies of the Cu-Ni system.[9] In that study, Eq. (4) was only useful for short times since the 8-μm Ni plating could be considered as infinite only as long as the free surface remained as pure Ni. This proved to be a severe limitation on the choice of both experimental diffusion times and temperatures even for thick film systems. Consequently, a more general form was developed which gave excellent results for finite platings on infinite substrates.[10]

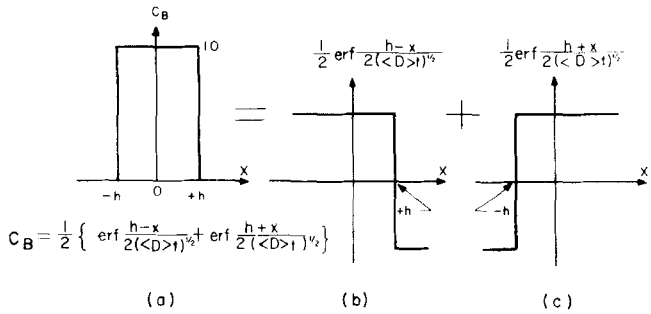

FIG. 1. Initial distribution of plating (a) and its two error function parts (b) having origins at $x = h$, and (c) with an origin at $x = -h$.

A solution of the finite plating problem may be found in Crank[5] provided D is constant. This can be obtained rigorously from first principles. A free surface is allowed for by constructing an image space which is a reflection of the concentration distribution within the specimen at the free surface. Figure 1(a) illustrates the initial distribution of solute in an infinite solvent for both specimen and image spaces. In the linear form of Fick's second law, the solute distribution can be determined by integrating over infinitesimal planar sources in the range $-h \le x \le h$ with x having its origin at the surface. The range of practical importance is, of course, limited only to positive values of x or specimen space and is given by

$$C_B = \tfrac{1}{2}C_0\left(\mathrm{erf}\frac{h-x}{2(\langle D\rangle t)^{1/2}} + \mathrm{erf}\frac{h+x}{2(\langle D\rangle t)^{1/2}}\right). \tag{6}$$

The first error function has an origin in specimen space ($x = h$), while the second has its origin in image space ($x = -h$). For short times, the second error function becomes unity and Eq. (6) is equivalent to Eq. (5) if the origin is shifted, i.e., $y = x - h$.

In a later development, it is helpful to recognize that Eq. (6) can be written in terms of two solutions to semi-infinite problems similar to that given by Eq. (4). An examination of Figs. 1(b) and 1(c) illustrates that the sum of these initial distributions gives the curve of Fig. 1(a). Consequently, solutions to the semi-infinite problems are represented by

$$\tfrac{1}{2}C_0\,\mathrm{erf}(\nu_1/\langle D\rangle^{1/2}), \quad \nu_1 = \frac{h-x}{2t^{1/2}}, \tag{7a}$$

and

$$\tfrac{1}{2}C_0\,\mathrm{erf}(\nu_2/\langle D\rangle^{1/2}), \quad \nu_2 = \frac{h+x}{2t^{1/2}}. \tag{7b}$$

The sum of Eqs. (7a) and (7b) is equal to Eq. (6) which can therefore be written by inspection. Since each error function separately satisfies Fick's second law, the sum is also a solution.

An analogous approach is used to approximate the nonlinear solution to Fick's second law [Eq. (1)]. Here it is assumed that one can superimpose two nonlinear solutions each of which is the solution to the corresponding semi-infinite problem. These solutions are

$$\tfrac{1}{2}C_0 I(\nu_1/\infty), \tag{8a}$$

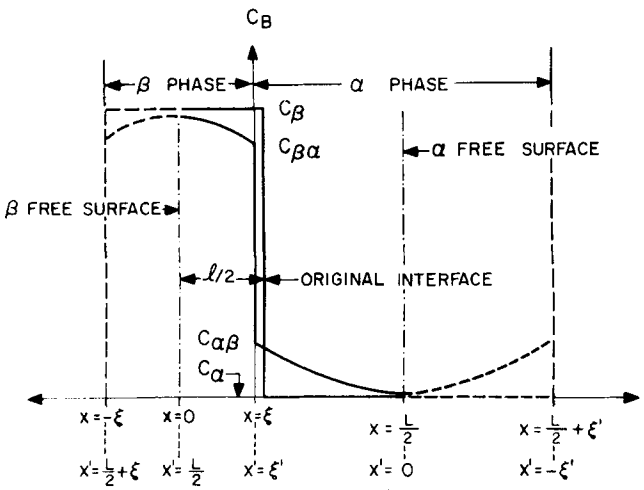

FIG. 2. Schematic representation of composition profile for finite two-phase system (solid line) or one period of a doubly infinite periodic system (solid + dashed line). For a finite system, $\frac{1}{2}l$ is the original plating thickness of β, $\frac{1}{2}L$ is the total thickness of $\beta+\alpha$, and $x=\xi$ locates the interface. Distance scale x has its origin at the center of β and is positive to the right, while x' has its origin in the center of α and is positive to the left.

and

$$\tfrac{1}{2}C_0 I(\nu_2/\bar{\infty}), \tag{8b}$$

which may be associated with Figs. 1(b) and 1(c) or Eqs. (7a) and (7b), respectively. The two integral functions are representable by a single form, i.e.,

$$I(s/\bar{\infty}) = 2\,\frac{I_0(s/\bar{\infty})}{I_0(\infty/\bar{\infty})} - 1, \tag{9}$$

where

$$I_0(s/\bar{\infty}) = \int_{-\infty}^{s} \frac{1}{D(C)} \exp\left(-\int_{-\infty}^{s'} \frac{2s''}{D(C)}\,ds''\right) ds' \tag{10}$$

and s is the variable ν_1 or ν_2 depending upon whether $I(\nu_1/\bar{\infty})$ or $I(\nu_2/\bar{\infty})$ is to be evaluated. The more general solution is

$$C_B = \tfrac{1}{2}C_0[I(\nu_1/\bar{\infty}) + I(\nu_2/\bar{\infty})]. \tag{11}$$

In the limit where $D(C) \to$ const, Eq. (11) $\to$ Eq. (6). The high degree of accuracy of this form has already been reported.[10]

III. TWO-PHASE SOLUTIONS

A. Constant D

1. Two finite phases

The single-phase solutions presented in Secs. I and II will provide a basis for approximate solutions to the two-phase diffusion-controlled planar moving interface problem. Several useful forms are given for finite semi-infinite cases, and constant as well as variable diffusion coefficients. In each case, the system is assumed to be conservative since it does not lose or gain material through the free surfaces.

The solid curve of Fig. 2 illustrates the composition profiles for β and α phases as well as the composition discontinuity at the interface for a typical finite diffusion couple. The specimen extends from $x=0$ to $\frac{1}{2}L$, while the dashed lines extend into the image space for each phase. Also, the positions at $x=0$ and $x=\frac{1}{2}L$ locate the free surfaces for a finite composite. The solution to this problem is equally valid for an infinite composite which is periodic (see Fig. 2 solid and dashed lines for one period). Extensive calculations on the interface position have already been carried out on this problem using a variable grid finite-difference approach[2] and these offer a convenient check on the closed-form solutions presented here. Unfortunately, these results assume the diffusion coefficients to be constant and no comparable calculations were carried out for composition-dependent coefficients. It will be assumed that the interface is not a hard reflector of diffusing atoms but rather a soft absorber. On the other hand, a free surface behaves as a hard reflector since atoms are not permitted to escape the solid into the vapor phase. This is accounted for by constructing images of each phase. Each phase is treated separately and interacts at the planar interface. The two-phase solution is constructed from single-phase solutions which are made to satisfy the boundary and initial conditions assuming that the interface position is quasistationary. For most binary systems this appears to be an excellent approximation.

Proceeding on this basis, the β-phase solution satisfying the surface condition ($\partial C/\partial x = 0$) and the boundary condition at the interface is represented by

$$C_B = C_\beta - (C_\beta - C_{\beta\alpha})\left(\operatorname{erfc}\frac{\xi+x}{2(D_\beta t)^{1/2}} + \operatorname{erfc}\frac{\xi-x}{2(D_\beta t)^{1/2}}\right) \times \left(1+\operatorname{erfc}\frac{\xi}{(D_\beta t)^{1/2}}\right)^{-1}, \tag{12}$$

and for the α phase

$$C_B = C_\alpha - (C_\alpha - C_{\alpha\beta})\left(\operatorname{erfc}\frac{x'+\xi'}{2(D_\alpha t)^{1/2}} + \operatorname{erfc}\frac{\xi'-x'}{2(D_\alpha t)^{1/2}}\right) \times \left(1+\operatorname{erfc}\frac{\xi'}{(D_\alpha t)^{1/2}}\right)^{-1}, \tag{13}$$

where C_β and C_α are the initial compositions of β and α, $C_{\beta\alpha}$ and $C_{\alpha\beta}$ are the compositions of β and α at the interface, and ξ and ξ' are the instantaneous thicknesses of β and α with $\xi+\xi'=\frac{1}{2}L$. The origin of x is at the β free surface and increases to the right, x' has an origin at the α surface and increases to the left, while D_β and D_α are the respective constant diffusion coefficients. Equations (12) and (13) are expressed in terms of the error function complement, i.e., erfcz = 1 − erfz. The interface position ξ is determined by requiring that the composite always conserves B atoms. Equations (12) and (13) may be integrated and set equal to the initial amount of element B giving

$$\frac{l}{2(D_\beta t)^{1/2}} = r_1 - \frac{2}{\sqrt{\pi}}\left[\frac{C_\beta - C_{\beta\alpha}}{C_\beta - C_\alpha}\,U(r_1) - \frac{C_{\alpha\beta} - C_\alpha}{C_\beta - C_\alpha}\left(\frac{D_\alpha}{D_\beta}\right)^{1/2} U(r_2)\right], \tag{14}$$

where $r_1 = \xi/(D_\beta t)^{1/2}$, $r_2 = (\frac{1}{2}L - \xi)/(D_\alpha t)^{1/2}$, and

$$U(r) = [1 - \exp(-r^2) + \sqrt{\pi}\,r\,\operatorname{erfc} r]/(1+\operatorname{erfc} r). \tag{15}$$

The interface position ξ is obtained from Eq. (14) by first selecting "t" and determining the value of ξ which satisfies the equation by trial and error. It is obvious that the concentration parameters, diffusion coefficients and sample thickness must be known if ξ is to be evaluated.

2. Semi-infinite case with infinite substrate

The semi-infinite problem with an infinite α substrate has already been considered.[3,4] However, the concentration profiles for this case are obtained from Eq. (12) and by noting that $\xi' - x' = x - \xi$ with $\xi' \to \infty$. Equation (13) becomes

$$C_B = C_\alpha - (C_\alpha - C_{\alpha\beta}) \operatorname{erfc} \frac{x-\xi}{2(D_\alpha t)^{1/2}} \tag{16}$$

and the corresponding transcendental equation for ξ is

$$\frac{t}{2(D_\beta t)^{1/2}} = r_1 - \frac{2}{\sqrt{\pi}} \left[\frac{C_\beta - C_{\beta\alpha}}{C_\beta - C_\alpha}\ U(r_1) - \frac{C_{\alpha\beta} - C_\alpha}{C_\beta - C_\alpha} \left(\frac{D_\alpha}{D_\beta}\right)\right] \tag{17}$$

since $U(r_2) \to 1$ in Eq. (14).

B. Variable D (C)

1. Two finite phases

The two-phase solutions for constant D are readily extended to allow for a variable interdiffusion coefficient. These are of the same form as those used to describe a single phase, i.e.,

$$C_B = A + B[I(\nu_1/0) + I(\nu_2/0)], \tag{18}$$

where A and B are determined such that the boundary conditions are always satisfied. The integral functions associated with each of the phases α and β are modifications of Eq. (9) with

$$I_\beta(s/0) = \frac{I_{0\beta}(s/0)}{I_{0\beta}(\nu_\xi/0)} \tag{19}$$

for the β phase, and $I_{0\beta}$ has the same form as Eq. (10) but with a lower limit of $s = 0$, an upper limit given by $\nu_\xi = \xi/t^{1/2}$, and $D(C) = D_\beta(C)$. Again, "s" is either $\nu_1 = (\xi - x)/2t^{1/2}$ or $\nu_2 = (\xi + x)/2t^{1/2}$. The integral functions associated with ν_1 and ν_2 for the β phase are integrated only over β-phase material. For $-\xi \le x \le \xi$, ν_1 and ν_2 extend over the ranges $0 \le \nu_1 \le \xi/t^{1/2}$, and $0 \le \nu_2 \le \xi/t^{1/2}$ which includes β-image and specimen space. The β-phase solution may be approximated by

$$C_B = C_\beta - \frac{C_\beta - C_{\beta\alpha}}{1 + \operatorname{erfc} \nu_\xi/D_{\beta\alpha}^{1/2}} \left[2 - \operatorname{erf}\left(\frac{\nu_\xi}{D_{\beta\alpha}^{1/2}}\right) I_\beta(\nu_1/0) - \operatorname{erf}\left(\frac{\nu_\xi}{D_{\beta\alpha}^{1/2}}\right) I_\beta(\nu_2/0),\right] \tag{20}$$

It is obvious that as $D(C)$ approaches $D_{\beta\alpha}$, a constant, Eq. (20) must approach Eq. (12) as a limit. This can be seen after considering the following limits

$$I_\beta(\nu_1/0) = \left.\frac{I_{0\beta}(\nu_1/0)}{I_{0\beta}(\nu_\xi/0)}\right|_{D(C)\to D_{\beta\alpha}} \to \frac{\operatorname{erf}\nu_1/D_{\beta\alpha}^{1/2}}{\operatorname{erf}\nu_\xi/D_{\beta\alpha}^{1/2}}.$$

A similar limit is obtained for the second term

$$I_\beta(\nu_2/0)\Big|_{D(C)\to D_{\beta\alpha}} \to \frac{\operatorname{erf}\nu_2/D_{\beta\alpha}^{1/2}}{\operatorname{erf}\nu_\xi/D_{\beta\alpha}^{1/2}}.$$

For $t \to 0$, Eq. (20) must go to C_β within β. As $t \to 0$, ν_ξ, ν_1, and $\nu_2 \to \infty$ causing the right-hand term of Eq. (20) to vanish giving C_β, the initial concentration. For $t \neq 0$ and $x = \xi$, one obtains $\nu_1 = 0$, $\nu_2 = \nu_\xi$ resulting in $I_\beta(0/0) = 0$, $I_\beta(\nu_\xi/0) = 1$ for the respective integral functions. As a consequence, Eq. (20) reduces to $C_{\beta\alpha}$ at the interface.

The corresponding expression for a finite α phase is representable by an analogous equation. In this case, the origin along the x axis is taken at the α free surface (see Fig. 2) with these values designated by $x' = \frac{1}{2}L - x$.

The concentration in α is given by

$$C_B = C_\alpha - \frac{C_\alpha - C_{\alpha\beta}}{1 + \operatorname{erfc}\nu'_{\xi'}/D_{\alpha\beta}^{1/2}} \left(2 - \operatorname{erf}\frac{\nu'_{\xi'}}{D_{\alpha\beta}^{1/2}}\ I_\alpha(\nu'_1/0) - \operatorname{erf}\frac{\nu'_{\xi'}}{D_{\alpha\beta}^{1/2}}\ I_\alpha(\nu'_2/0),\right) \tag{21}$$

with $\nu'_1 = (\xi' - x')/2t^{1/2}$, $\nu'_2 = (\xi' + x')/2t^{1/2}$, and $\nu'_{\xi'} = \xi'/t^{1/2}$. Also, $I_\alpha(s/0) = I_{0\alpha}(s/0)/I_{0\alpha}(\nu'_{\xi'}/0)$ and "s" is either ν'_1 or ν'_2. The integral function $I_{0\alpha}(s/0)$ is given by Eq. (10) with $D(C) = D_\alpha(C)$. Equation (21) reduces to C_α within the α phase for $t \to 0$ and to $C_{\alpha\beta}$ for $x' = \xi'$.

2. Finite β and infinite α phase

If the β phase is finite and α is infinite, the composition distribution for α can be further simplified to

$$C_B = C_{\alpha\beta} - (C_{\alpha\beta} - C_\alpha) \frac{I_{0\alpha}(\nu_3/0)}{I_{0\alpha}(\infty/0)}, \tag{22}$$

with $\nu_3 = \overline{\nu_1} = (x - \xi)/2t^{1/2}$ introduced as the variable. The mathematical form for β remains unaltered and is still represented by Eq. (20).

3. Interface position by mass balance

Two methods have been employed by the authors to locate the interface position ξ. The first approach made use of the typical interface mass balance equation, while the second located the interface so as to conserve the total amount of each element. Although the conservation approach is preferred, the interface mass balance approach will also be described. This is based upon the equation

$$(C_{\beta\alpha} - C_{\alpha\beta}) \frac{d\xi}{dt} = (J_\beta - J_\alpha)_{x=\xi}$$

which requires Fick's first law to calculate the respective interface fluxes J_β and J_α giving

$$J_\beta = \frac{(C_\beta - C_{\beta\alpha}) \operatorname{erf}\nu_\xi/D_{\beta\alpha}^{1/2}}{2t^{1/2}(1 + \operatorname{erfc}\nu_\xi/D_{\beta\alpha}^{1/2})} \left(\frac{1 - \exp(-\int_0^{\nu_\xi}(2s/D_\beta)\,ds)}{I_{0\beta}(\nu_\xi/0)}\right)$$

and

$$J_\alpha = \frac{C_{\alpha\beta} - C_\alpha}{2t^{1/2}(I_{0\alpha}(\infty/0)}.$$

The flux J_α can readily be calculated for a finite thickness; however, our prior experience has only been with an infinite α phase. Consequently, the calculation is restricted to the semi-infinite case. Substituting the fluxes into the interface mass balance equation gives the following

$$(C_{\beta\alpha} - C_{\alpha\beta}) \frac{d\xi}{dl} = \frac{f(\nu_\xi)}{2l^{1/2}}, \tag{23}$$

where

$$f(\nu_\xi) = \left\{ (C_\beta - C_{\beta\alpha}) \left[1 - \exp\left(- \int_0^{\nu_\xi} \frac{2\nu}{D_\beta}\, d\nu \right) \right] \operatorname{erf} \frac{\nu_\xi}{D_{\beta\alpha}^{1/2}} \right\}$$
$$\times \left[\left(1 + \operatorname{erfc} \frac{\nu_\xi}{D_{\beta\alpha}^{1/2}} \right) \int_0^{\nu_\xi} \frac{1}{D_\beta} \exp\left(- \int_0^{\nu} \frac{2\nu}{D_\xi}\, d\nu \right) d\nu \right]^{-1}$$
$$- (C_{\alpha\beta} - C_\alpha) \left[\int_0^{\infty} \frac{1}{D_\alpha} \exp\left(- \int_0^{\nu} \frac{2\nu}{D_\alpha}\, d\nu \right) d\nu \right]^{-1}.$$

Equation (23) can be written in terms of ξ and ν_ξ alone and integrated to give the following

$$2\xi = l \exp \int_\infty^{\nu_\xi} \frac{f(\nu_\xi)}{\nu_\xi [f(\nu_\xi) - (C_{\beta\alpha} - C_{\alpha\beta})\, \nu_\xi]}\, d\nu_\xi . \tag{24}$$

Composition profiles C_B are obtained for each phase from an iterative scheme which makes use of Eqs. (20), (22), and (24). The procedure is sequential in time, numerically cumbersome, but requires much less computer time than finite-difference calculations because of the rapid convergence of the integral functions. These iterative calculations are initiated using more approximate functions obtainable in the limit of constant D. The procedure is similar but more complicated than that described in Sec. II and will not be considered any further.

4. Interface position by conservation

An alternate approach is preferred for obtaining the interface position ξ. This makes use of the conservation principle which requires that the interface be located such that component B is always conserved. With this approach, Eqs. (20) and (21) are integrated to obtain the total amount of B and this is adjusted to give the original amount by varying the value of ξ. Solutions need not be sequential in time. Consequently, the computer time is the same for short and long diffusion times. All subsequent calculations in this paper were obtained using the conservation approach.

5. Volume changes

The diffusion calculations are, for convenience, carried out using equations which are based on the assumption that $\bar{V}_1 = \bar{V}_2$, where $\bar{V}_i$ is the partial molar volume of component i. The same equations can be extended to cover the case of ideal mixing ($\bar{V}_1 \neq \bar{V}_2$, but with each $\bar{V}_i$ constant) if volume fraction is employed as the concentration unit.[11] It has been shown that the customary diffusion equations can be used with this concentration unit, including the Darken analysis for intrinsic diffusion coefficients.[12] Consequently, C will be treated as the volume fraction of one of the diffusing components whenever significant volume changes are observed.

IV. ACCURACY OF TWO-PHASE SOLUTIONS

A. Constant D

The mathematical forms that have been developed for the concentration in each phase are approximations to Fick's second law. Consequently, to determine the interface position, one can require that the interface mass balance equation be satisfied or that the system be conservative. For special cases involving either very short times or long times, it can be demonstrated that if the first condition is applied, the solutions are not strictly conservative. On the other hand, if the solutions are made to be conservative, they become approximate with respect to the interface mass balance equation. Another convenient check, which is the only one available for intermediate times, involves the use of finite-difference calculations (F-D). Although it is tempting to consider F-D calculations to be exact when the proper grid is used, difficulties may be encountered here also. Application of an interface mass balance equation requires accurate values of the composition gradients on either side of the interface. If the composition profiles are highly nonlinear, the usual linear approximations are not adequate unless a very small grid size is used which often results in excessive run times. A practical alternative is to make use of a conservation criterion to locate the interface position ξ. However, this too requires approximations. In this section, our results will be compared with exact solutions over limited time periods as well as with F-D calculations.

Before comparing these solutions, it is convenient to define three stages of development in terms of the boundary conditions. For short times, the two-phase system can be considered as doubly infinite. This will be defined as stage I and an exact solution is available provided D is constant for each phase. For thin coatings of β on an α substrate, this stage can be very short and difficult to attain experimentally. An intermediate stage (II) includes that interval of time over which the surface composition $C_B(x = 0, l)$ varies in the range $C_\beta \quad C_B \quad C_{\beta\alpha}$. It is complicated because the interface fluxes depend upon the interface position. For most cases, one finds that the interface moves by less than 20% of the original β-phase thickness throughout stages I and II. (More is possible if the solubility of the β phase is large.) During stage III, the β phase has a uniform composition and therefore does not contribute a flux for interface motion. In this stage, diffusion in the α phase is the controlling factor.

Interface motion through stage I is parabolic and expressible in the conventional form $\xi = \frac{1}{2}l + 2b_1(D_\alpha l)^{1/2}$. This is a consequence of the doubly infinite boundary condition. The constant coefficient of the time-dependent term b_1 is given rigorously by the following transcendental equation[6]

$$b_1 = \frac{1}{\sqrt{\pi}} \left[\frac{C_\beta - C_{\beta\alpha}}{C_{\beta\alpha} - C_{\alpha\beta}} \left(\frac{D_\beta}{D_\alpha} \right)^{1/2} \frac{\exp[-(b_1\phi)^2]}{1 + \operatorname{erf} b_1\phi} \right.$$
$$\left. - \frac{C_{\alpha\beta} - C_\alpha}{C_{\beta\alpha} - C_{\alpha\beta}} \frac{\exp(-b_1^2)}{\operatorname{erfc} b_1} \right] \tag{25}$$

with $\phi = (D_\alpha / D_\beta)^{1/2}$. A similar equation can be obtained from Eq. (17) after allowing β to become infinite, i.e.,

$$b_1 = \frac{1}{\sqrt{\pi}} \left[\frac{C_\beta - C_{\beta\alpha}}{C_{\beta\alpha} - C_{\alpha\beta}} \left(\frac{D_\beta}{D_o} \right)^{1/2} \left(\frac{C_{\beta\alpha} - C_{\alpha\xi}}{C_\beta - C_\alpha} \right) \right.$$
$$\left. - \frac{C_{\alpha\beta} - C_\alpha}{C_{\beta\alpha} - C_{\alpha\beta}} \left(\frac{C_{\beta\alpha} - C_{\alpha\beta}}{C_\beta - C_\alpha} \right) \right] . \tag{26}$$

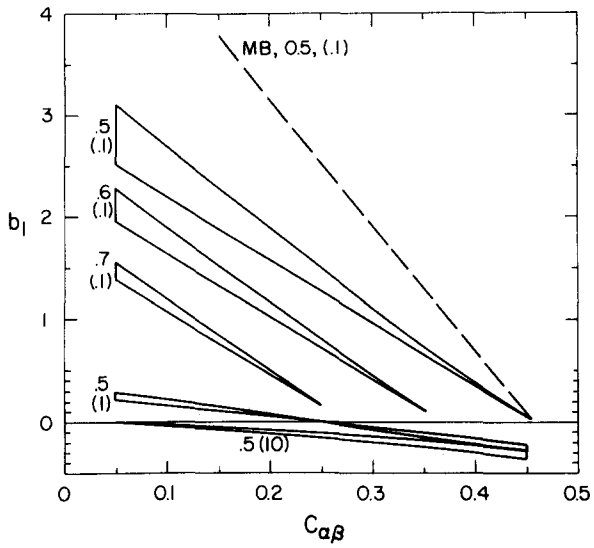

FIG. 3. Comparison of b_1 versus $C_{\alpha\beta}$ as determined by the exact expression [Eq. (25)] and the conservation approximation [Eq. (26)]. The upper curve in each pair is the exact calculation, while the lower is obtained from Eq. (26). Each pair is designated by the gap $C_{\beta\alpha} - C_{\alpha\beta}$ (0.5, 0.6, 0.7) and $(D_\alpha/D_\beta)^{1/2}$ is given in parentheses, i.e., (0.1), (1), and (10). The upper dashed curve was calculated using interface mass balance for a gap of 0.5 and $(D_\alpha/D_\beta)^{1/2} = 0.1$.

Equation (26) is obtained from a conservation argument and gives approximately the correct interface flux balance. To determine the accuracy of Eq. (26), it was examined relative to Eq. (25) for a range of system variables. These are given in Fig. 3 and 4. For each plot of b_1, the gap $C_{\beta\alpha} - C_{\alpha\beta}$ was held constant and $C_{\alpha\beta}$ was allowed to vary. Figure 3 illustrates those cases where the $C_{\beta\alpha} - C_{\alpha\beta}$ gap lies between 0.7 and 0.5 which is on the large side for most binary eutectic systems. In these cases, the error in b_1 extends from 12 to 20% with the largest error corresponding to 0.5. Figure 4 illustrates larger composition gaps from 0.7 to 0.9. For gaps in the range 0.8 to slightly less than unity, b_1 is accurate to better than 10% with the highest accuracy corresponding to the largest gaps. The accuracy in ξ is better than what the percentages would at first indicate since the interface movement is generally less than 20% of the initial β-phase thickness. With the 20% number, ξ should be accurate to within 4% for all cases given in Fig. 3 and within 2% of those considered in Fig. 4. These results demonstrate that the conservation Eq. (26) underestimates interface movement, and leads to the largest errors when the quantities $C_\beta - C_{\beta\alpha}$ together with D_β/D_α are both large. Under these conditions, the interface moves into the substrate by the largest amount before reversing. The upper curve of Fig. 3 illustrates the relatively poor approximation obtained from the interface mass balance equation. It can be seen that the discrepancy is about four times larger if the interface mass balance criterion is used and is in a direction that overestimates the interface position ξ. This trend is also typical for all other gaps $C_{\beta\alpha} - C_{\alpha\beta}$.

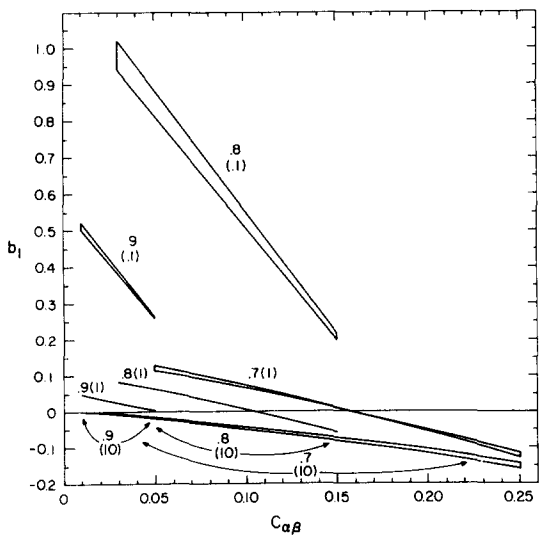

FIG. 4. Same as Fig. 3 but for $C_{\beta\alpha} - C_{\alpha\beta} = 0.7$, 0.8, and 0.9. Again, the upper curve for each pair is exact, while the lower is approximate.

The boundary conditions for stage III also result in parabolic interface motion such that $\xi = \frac{1}{2}l_3 + 2b_3[D_\alpha(t - t_0)]^{1/2}$, with $\frac{1}{2}l_3$ representing the interface position at the beginning of this stage ($t = t_0$). It has been assumed that the α substrate thickness is large relative to β. Otherwise, the interface would not move parabolically. Like stage I, the coefficient b_3 is independent of time and is rigorously given by

$$b_3 = -\frac{1}{\sqrt{\pi}} \frac{C_{\alpha\beta} - C_\alpha}{C_{\beta\alpha} - C_{\alpha\beta}} \frac{\exp(-b_3^2)}{\operatorname{erfc} b_3}, \tag{27}$$

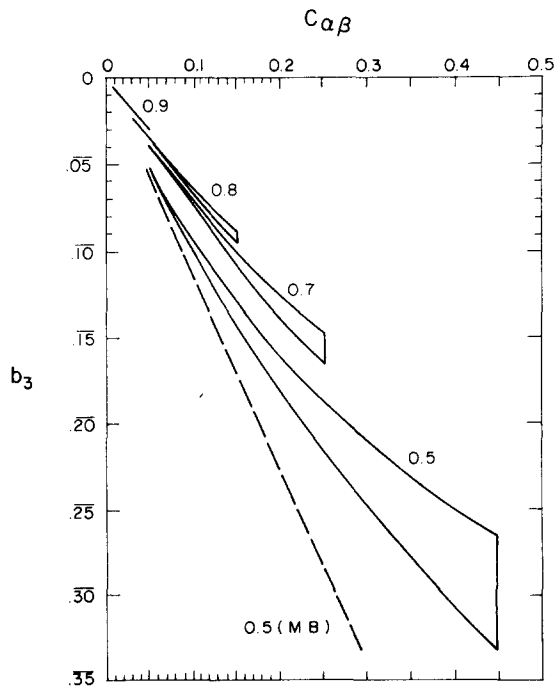

FIG. 5. Comparison of b_3 versus $C_{\alpha\beta}$ determined by the exact expression (Eq. 27) and the conservation approximation (Eq. 28). Lower curve in each pair is exact, while the upper is approximate. Gap size is designated for each pair. The lower dashed curve was calculated using interface mass balance for a gap of 0.5.

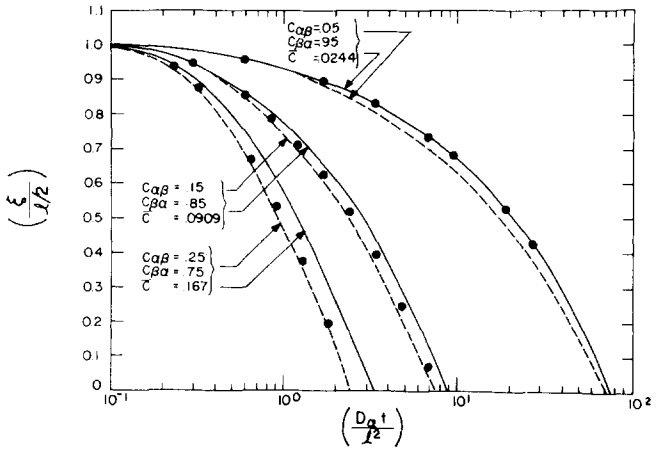

FIG. 6. Comparison between relative interface position calculated by F-D and Eq. (14). Solid line is determined from Eq. (14), while the dashed are F-D calculations by Tanzilli and Heckel (Ref. 2). The circles are F-D calculations by the authors. Gaps of $C_{\beta\alpha} - C_{\alpha\beta} = 0.9$ (upper curves), 0.7 (middle), and 0.5 (lower) are illustrated. Also, $D_\alpha = D_\beta$ const. $\bar{C}$ is the mean composition and is equal to l/L.

while the present conservation criterion gives

$$b_3 = -\frac{1}{\sqrt{\pi}} \frac{C_{\alpha\beta} - C_\alpha}{C_{\beta\alpha} - C_{\alpha\beta}} \frac{C_{\beta\alpha} - C_{\alpha\beta}}{C_{\beta\alpha} - C_\alpha} \tag{28}$$

and approximate agreement with the interface flux balance. Again, Eqs. (27) and (28) were examined over a range of system variables. Figure 5 illustrates various gap sizes from 0.5 to 0.9. For each pair, the lower curve corresponds to the exact result, Eq. (27), while the upper corresponds to Eq. (28). The maximum error introduced by Eq. (28) ranges from 20% for 0.5 and 2% for a 0.9 gap size. Also, for stage III, the interface position is independent of D_β and therefore the curves are independent of the ratio of diffusion coefficients. Stage III generally requires much larger times for completion than either I or II and the interface can move a distance comparable to the original β-phase thickness. Consequently, a 20% error in b_3 is likely to introduce a comparable error in ξ. (This is not the case for stage I.) Again, the lower curve for 0.5 (MB) illustrates the relatively large error introduced when the interface mass balance equation is employed for stage III.

Because stage II is intermediate between I and III, one might expect to find the accuracy for this more complicated stage to be characteristic of the bounding stages. stages. Since there are no exact solutions describing this stage, it was necessary to compare our results with F-D calculations already in the literature[2] which were obtained under various conditions using constant and equal diffusion coefficients. Figure 6 illustrates three plots of interface position calculated from Eq. (14) and compared with F-D calculations for all three stages. The circles are F-D calculations carried out by the authors that are somewhat higher than the literature values. A comparison between the two types of calculations demonstrates that the accuracy increases with $C_{\beta\alpha} - C_{\alpha\beta}$ giving end point values of about 18% (0.5), 7% (0.7), and 2% (0.9). To obtain these values, both sets of F-D calculations were averaged. These percentages agree very well with the values previously calculated for b_1 and b_3 during stages I and III.

Figure 7 illustrates an example in which interface reversal takes place. The conditions $C_\beta - C_{\beta\alpha} = 0.35$, $C_{\alpha\beta} - C_\alpha = 0.05$, $C_{\beta\alpha} - C_{\alpha\beta} = 0.60$, and $D_\alpha = D_\beta$, provide an initial β flux which is greater than the α flux. A significant difference was found between the upper F-D curve given in the literature and calculations based upon Eq. (14) that is outside of the anticipated error. Consequently, they were repeated using various grid sizes. The new values are plotted as circles. They are close to but slightly higher than the analytic form for stage I and appear to drop slightly below for stage III. A 3% error is found in ξ for stage I. This corresponds to a previously predicted error of about 15% in b_1 if it is recognized that the interface only moves by 18% for this stage. The upper dashed curve is not correct since it exceeds 1.54. This can be understood if one considers an extreme case having a very large D_β/D_α. Such an example would cause the β phase to extend with practically no loss of B atoms by diffusion into α. Therefore, by conservation, the largest possible displace-

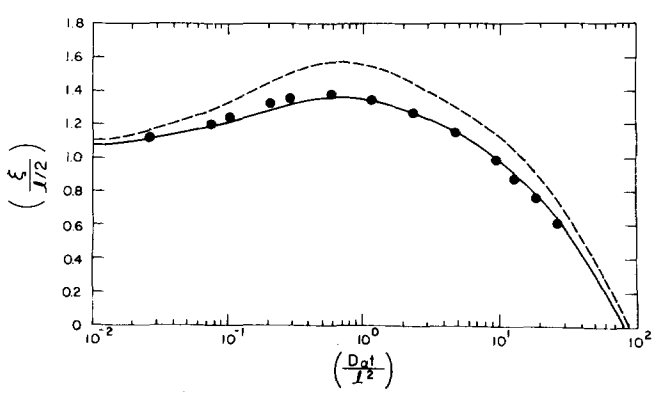

FIG. 7. Interface reversal with $C_\beta - C_{\beta\alpha} = 0.35$, $C_{\alpha\beta} - C_\alpha = 0.05$, $C_{\beta\alpha} - C_{\alpha\beta} = 0.6$, and $D_\alpha = D_\beta$. Solid line is determined from Eq. (14), the dashed lines are F-D calculations by Tanzilli and Heckel (Ref. 2), and the circles are F-D calculations by the authors.

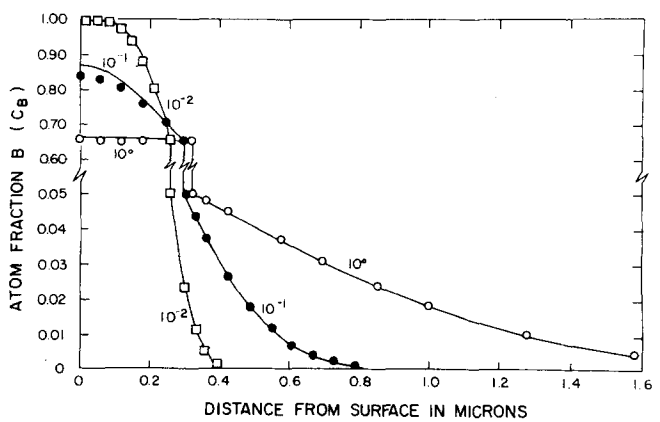

FIG. 8. Composition profiles corresponding to the scaled times $D_\alpha t/l^2 = 10^{-2}$, 10^{-1}, and 10^0 of Fig. 7. Solid curves were calculated from Eqs. (12)—(14) with points obtained from F-D calculations.

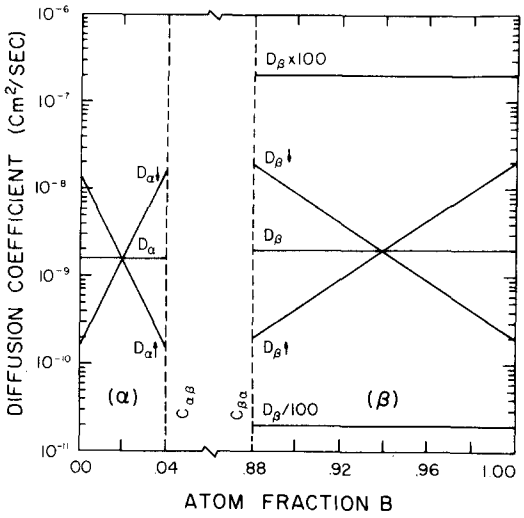

FIG. 9. Semilog plots of $D(C)$ which are used to obtain Figs. 10—14.

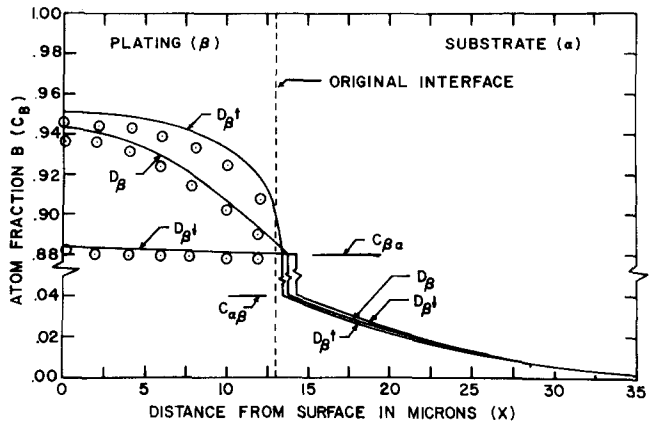

FIG. 11. Concentration profiles obtained from diffusion coefficients $D_\alpha - D_\beta\uparrow$, $D_\alpha - D_\beta\downarrow$, and $D_\alpha (=1.57\times10^{-9}) - D_\beta (=1.93\times10^{-9})$ after 0.1 h of diffusion. Refer to Fig. 9 for $D(C)$. Solid lines were obtained using Eqs. (20) and (22), while the points are from F-D calculations. Solubilities correspond to Ag-Cu at 750 °C.

ment for $\xi/\frac{1}{2}l$ is $C_\beta/C_{\beta\alpha} = 1.00/0.65 = 1.54$. The example illustrated in Fig. 7 is not such an extreme case since $D_\alpha = D_\beta$ and should give a maximum somewhat less than 1.4.

Three profiles calculated from Eqs. (12)—(14) and corresponding to the scaled times $D_\alpha t/l^2 = 10^{-2}$, 10^{-1}, and 10^0 of Fig. 7, are plotted in Fig. 8. The shortest time (10^{-2}) corresponds to the end of stage I, while 10^{-1} is halfway through stage II, and 10^0 is near the beginning of stage III. In this example, excellent agreement is found with our F-D calculations for the shortest and longest times. For stage II, the compositions are within 5% on the β side and in nearly perfect agreement for α.

B. Variable diffusion coefficient

The accuracy of Eqs. (20) and (22) will be examined using various forms for $D(C)$ and composition limits that correspond to the Ag-Cu system at 750 °C. This system will be discussed in considerable detail in the following paper. For a 13-μm Ag plating on a thick Cu substrate with $C_\beta - C_{\alpha\beta} = 0.12$, $C_{\alpha\beta} - C_\alpha = 0.04$, and $C_{\beta\alpha} - C_{\alpha\beta} = 0.84$, Figures 4 and 5 indicate that b_1 and b_3 should be within 8.4 and 1.4%, respectively. Assuming that the interface moves only 20% of the original β thickness, the absolute accuracy of ξ should be within 1.7% for these conditions. However, in these calculations, D has been assumed to be a constant and additional errors could result from variations in D. These may be considered by making comparisons with F-D calculations using diffusion coefficients illustrated in Fig. 9. A linear logarithmic form was used for convenience; however, any continuous curve may be used. In some cases, a constant coefficient is introduced since the resultant composition profiles provide better understood reference curves. Figures 10 and 11 were obtained by taking the following pairs: $D_\alpha - D_\beta/100$, $D_\alpha - D_\beta\times100$, and $D_\alpha - D_\beta\downarrow$, $D_\alpha - D_\beta\uparrow$, respectively. The central curves involving $D_\alpha - D_\beta$ with constant coefficients are repeated

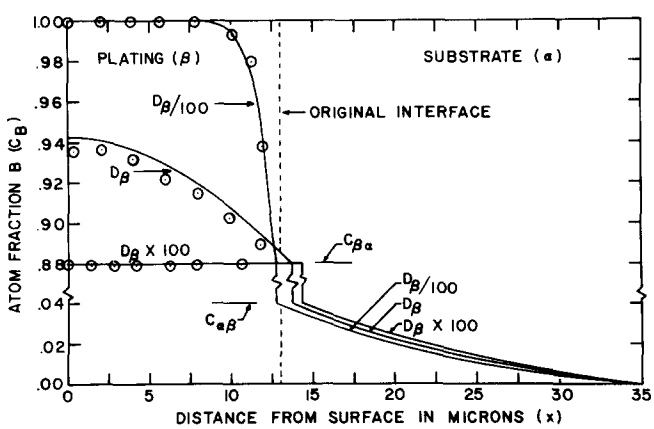

FIG. 10. Concentration profiles obtained from diffusion coefficients $D_\alpha - D_\beta/100$, $D_\alpha - D_\beta\times100$, and $D_\alpha (=1.57\times10^{-9}) - D_\beta - D_\beta (=1.93\times10^{-9})$ after 0.1 h of diffusion. Solid lines were obtained from Eqs. (20) and (22), while the points are from F-D calculations. Solubilities correspond to Ag-Cu at 750 °C.

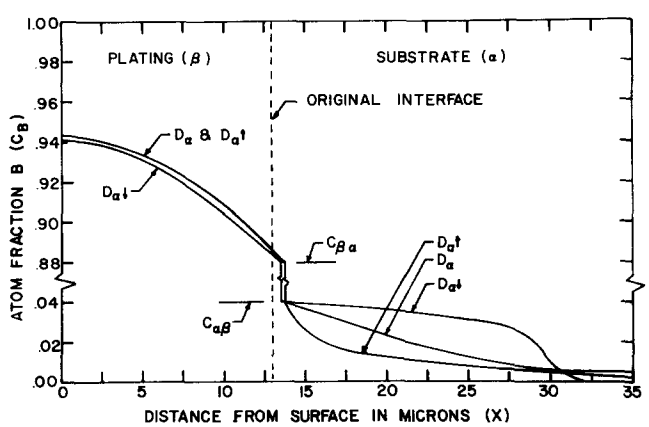

FIG. 12. Concentration profiles obtained from diffusion coefficients $D_\beta - D_\alpha\uparrow$, $D_\beta - D_\alpha\downarrow$, and $D_\alpha (=1.57\times10^{-9}) - D_\beta (=1.93\times10^{-9})$ after 0.1 h. Refer to Fig. 9 for $D(C)$. Solid lines were obtained from Eqs. (20) and (22). Solubilities correspond to Ag-Cu at 750 °C.

for a comparison. A comparison of Figs. 10 and 11 indicates that the F-D points do not show a striking discrepancy between profiles obtained with variable $D(C)$ and those for constant D. Allowing D to vary with composition reshapes the profiles, but in this example it does not introduce an additional discrepancy. All compositions and ξ values are within 1% despite the large variations in D which have been introduced.

Figures 10–12 represent the concentration profiles for various diffusion coefficients at $t = 0.1$ h. Figure 10 illustrates the changes in concentration profile as the constant D_β is increased or decreased by two magnitudes, keeping D_α constant. Since D_α is kept constant, the profiles in the α phase are about the same. The small variations result from changes in interface position. However, there is a significant difference in the β-phase concentration profiles. The $D_\beta/100$ profile is in stage I, while the D_β profile is in stage II and the $D_\beta \times 100$ profile corresponds to stage III. Thus, for $t = 0.1$ h, the β phase is in three different stages of development for the β diffusion coefficients considered. The F-D results for the α phase are identical with the present iterative solution (solid lines) and therefore the F-D points are not shown in these plots.

Figure 11 illustrates the changes in concentration profiles for the β diffusion coefficient shapes D_β, $D_\beta{}'$, and $D_\beta{}'$ (see Fig. 9), keeping D_α constant at 15.7×10^{-10} cm^2/sec. The profiles in the α phase are about the same with small variations arising from changes in the interface position. The profiles for the β phase are indicative of stage II for D_β and $D_\beta{}'$ cases, and close to the beginning of stage III for $D_\beta{}'$ case. The appropriate F-D results are shown as points for the β phase. Again, the F-D points for the α phase are not included because they are identical with the present iterative solution.

Consider now the concentration profile with $D_\beta{}'$ (see Fig. 11) where the maximum discrepancy is seen between the iterative and the F-D results. The analytic solution (solid line) is exactly conservative because the ξ was obtained by using the conservation principle so that the total amount of B is exactly 13.00 units (= plating thickness). However, the F-D solution for this case deviated slightly from conservation with 12.92 units of B material. Since the profiles for the α phase are identical with both calculations, the F-D profile must be lower than the analytic profile in the β phase. In fact, the total discrepancy between both the β profiles (Fig. 11) can be seen to be about 0.08 units, which is equal to the conservation error in the F-D calculations. Consequently, it can be concluded that the present iterative form is in excellent agreement with the F-D calculations.

Figure 12 illustrates the concentration profiles resulting from variations in the α-phase diffusion coefficients, keeping D_β constant at 19.3×10^{-10} cm^2/sec. Although it was possible to obtain reasonable curves from the iterative form, similar results could not be obtained from F-D calculations. The corresponding F-D results are not shown because they deviate from conservation by 9% and they contained troublesome oscillations making them unreliable. Since D_β is constant for the three cases shown, the concentration profiles for the β phase

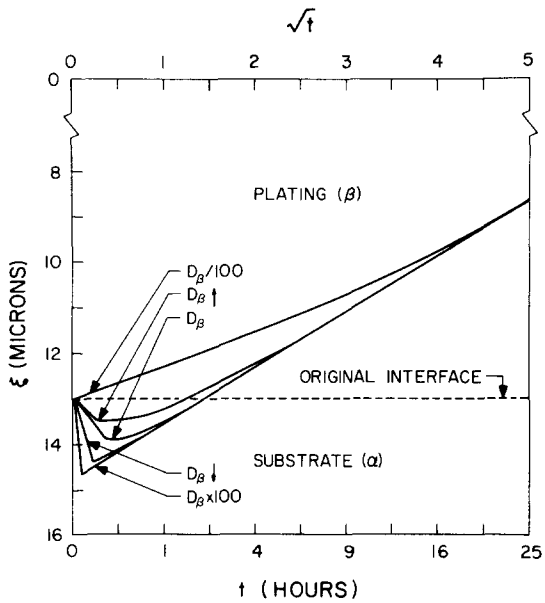

FIG. 13. Interface position versus $t^{1/2}$ for various shapes of $D_\beta(C)$ holding D_α constant at 1.57×10^{-9} cm^2/sec. Refer to Fig. 9 for $D(C)$. Plating thickness is 13 μm.

are about the same. The small variations are due to changes in the interface positions. Profiles on the α side are significantly different due to large variations introduced in the α diffusion coefficient. The interfacial diffusion coefficient $D_{\alpha\beta}$ (corresponding to $C_{\alpha\beta}$) is so high for the $D_\alpha{}'$ case that the concentration profile is virtually flat near the interface. On the other hand, for the $D_\alpha{}'$ case, the concentration in the interfacial region decreases sharply due to the relatively small $D_{\alpha\beta}$. The α concentration profile for constant D_α is intermediate between $D_\alpha{}'$ and $D_\alpha{}'$ as expected. Concentration gradients in the deep substrate can be similarly explained by differences in D for this region.

Figure 13 shows the interface position as a function of $t^{1/2}$ using the present iterative solution for five cases. Here D_α is kept constant at 15.7×10^{-10} cm^2/sec and D_β is allowed to vary (see Fig. 9). The interface position is plotted against $t^{1/2}$ so as to detect parabolic motion of the interface. The three stages of development within the β phase can be clearly seen for all examples. However, it is less obvious for $D_\beta/100$. The first straight-line portion going into the substrate represents stage I where the system can be treated to be doubly infinite. The final straight line is due to stage III where the β flux is zero and it therefore does not contribute to interface motion. The intermediate curve joining these two straight lines is due to stage II where the surface concentration varies between C_β and $C_{\beta\alpha}$. In all the cases, it can be seen that as $D_{\beta\alpha}$ (at $C_{\beta\alpha}$) increases, the time span for stage II decreases and the time span for stage III increases. For longer times ($t \gtrsim 16$ h) all cases give rise to the same ξ and the interface moves parabolically with time.

Figure 14 shows the interface position plotted against $t^{1/2}$ for three shapes of the α-phase diffusion coefficient. Here D_β is kept constant at 19.3×10^{-10} cm^2/sec and D_α is allowed to vary (see Fig. 9). In all three cases, the

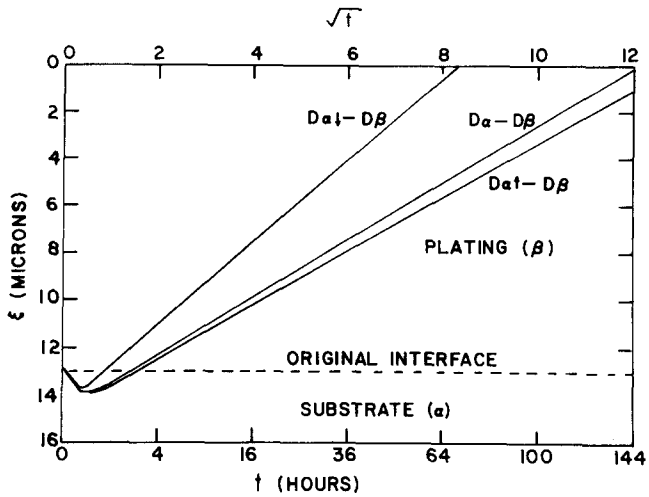

FIG. 14. Interface position versus $t^{1/2}$ for various shapes of $D_\alpha(C)$ holding D_β constant at $1.93 \cdot 10^{-4}$ cm^2/sec. Refer to Fig. 9. Plating thickness is 13 μm.

interface initially moves into the substrate parabolically then changes its direction and moves toward the surface. Stage III motion is parabolic even though the diffusion coefficient for the α phase is not constant.

In comparing Figs. 13 and 14 one finds that only $D_\beta/100$ (Fig. 13) does not lead to interface reversal even though $D_{\alpha'}$ evaluated at $C_{\alpha\beta}$ is larger than D_β. The interface flux balance of stage I determines whether reversal will occur. Since short times are involved, the α diffusion zone is relatively small as compared with the large penetration of stage III. Consequently, this small penetration introduces a coupled interaction in which the entire range of compositions can influence the interfacial α flux. The tendency for interface reversal in this example can be predicted from the following inequality

$$\ln D_\beta \quad \langle \ln D_\alpha \rangle$$

in which $\langle \ln D_\alpha \rangle$ is an over-all average of $\ln D_\alpha$. If this is satisfied reversal will take place since the initial gradient is largely determined by $C_\beta - C_{\beta\alpha}$ and $C_{\alpha\beta} - C_\alpha$. During stage III, the α zone is sufficiently large that only a fraction of its over-all size influences motion, i.e., only those compositions near $C_{\alpha\beta}$. This sensing tendency at the interface can be seen in Fig. 14 where the velocity $d\xi/dt$ is dependent upon the relative values of D_α at (or near) $C_{\alpha\beta}$. In this case, the inequality $D_{\alpha'} \quad D_\alpha \quad D_{\alpha'}$ is in accord with the respective decrease in velocities.

V. DISCUSSION

Approximate iterative solutions are given for planar single- and two-phase diffusion problems that allow the diffusion coefficient to vary with composition in finite and semifinite systems. They are usable for any continuous variation of $D(C)$ within each phase, and it is not necessary to assume that $D(C)$ can be fitted to a special function such as a power series or an exponential function. Consequently, $D(C)$ could be actual experimental data. If this is known, the composition profile can be determined directly for any time within the first three stages of diffusion. The approximations are based upon an integral equation first proposed by Boltzmann that is solved by a rapidly converging iterative procedure. The results generally provide an excellent check with F-D calculations whenever the latter are conservative and do not oscillate. Equations (11) and (20)–(22) should be especially useful for thin or thick film diffusion problems. For these problems, the computer time required for F-D calculations is often prohibitive with run times that approach the diffusion times.

Equations (20)–(22) have been used together with the conservation criterion. This allows the interface position ξ to be determined as well as a composition profile for each phase. Although Figs. 3–5 apply to the more restrictive case of constant diffusion coefficients, they also provide an indication of the errors associated with problems in which the diffusion coefficient varies with concentration. These demonstrate that the accuracy increases with decreasing solubility for both phase or for increasing gap size $C_{\beta\alpha} - C_{\alpha\beta}$.

Equation (11) has been used to determine $D(C)$ for a single-phase system consisting of a finite plating on a thick substrate. The system began as a pure element at the free surface and was diffused to give a surface composition of about 50%. Diffusion coefficients were obtained by fitting the experimental profile.[13] A typical trial and error fitting begins by first determining a constant D which roughly describes the over-all extent of the diffused region. The shape of the composition profile is not of major concern at this point. For the first refinement, a better fitting of the shape is attained by increasing $D(C)$ where the composition gradient must be reduced and decreasing it where the gradient must be increased. These adjustments in $D(C)$ are usually carried out using semilogarithm plots with the average of $\ln D$ approximately corresponding to the original value of D. Refinements in the shape of $D(C)$ are continued until the composition profile is in agreement with the measured curve. Since the interative solution only takes seconds of computer time, curves can be fitted quickly by using a graphics computer terminal. All iterative solutions checked by F-D calculations were in excellent agreement provided that the latter solutions were conservative.

The determination of $D_\alpha(C)$ and $D_\beta(C)$ for two phase problems is identical with the single-phase procedure except two curves must be obtained as well as the interface position. If the system is finite, Eqs. (20) and (21) are used, while if one phase is infinite, Eq. (22) may be substituted for Eq. (21). The fitting procedure for $D_i(C)$ is best carried out from near the end of stage I to about the middle of stage II, but before either profile has flattened. For most real eutectic systems, very good results can be expected over this time period. The following paper illustrates the application of Eqs. (20) and (22) to experimental data obtained for the Ag-Cu system.

Additional details on the numerical analysis asso-

ciated with Eqs. (11) and (20)—(22) as well as the computer programs will be made available in the VPI& SU College of Engineering report entitled "Iterative and Finite Difference Computer Programs for Diffusion in Single and Two Phase Systems" distributed by the National Technical Information Service.

ACKNOWLEDGMENT

The authors are grateful to the National Science Foundation for funding this research.

[1]A.G. Guy and H. Oikawa, Trans. AIME **245**, 2293 (1969).
[2]R.A. Tanzilli and R.W. Heckel, Trans. AIME **242**, 2313 (1968).
[3]J. Unnam and C.R. Houska, Scr. Metall. **8**, 61 (1974).
[4]J. Unnam and C.R. Houska, Scr. Metall. **8**, 801 (1974).
[5]J. Crank, *The Mathematics of Diffusion* (Oxford U.P. London, 1964).
[6]W. Jost, *Diffusion in Solids, Liquids and Gases* (Academic, New York, 1960).
[7]H.S. Carslaw and J.C. Jaeger, *Conduction of Heat in Solids* (Oxford U.P., London, 1947).
[8]L. Boltzmann, Ann. Phys. (Leipzig) **53**, 959 (1894).
[9]D.R. Tenney, J.A. Carpenter, and C.R. Houska, J. Appl. Phys. **41**, 4485 (1970).
[10]C.R. Houska and J. Unnam, Scr. Metall. **8**, 509 (1974).
[11]A.G. Guy, R.T. DeHoff, and C.B. Smith, ASM Trans. Q. **61**, 314 (1968).
[12]R.L. Fogelson, Fiz. Met. Metalloved. **19**, 212 (1965).
[13]G. Subbaraman, M.S. thesis (Virginia Polytechnic Institute and State University, Blacksbury, Virginia, 1974) (unpublished).